Available online at www.sciencedirect.com
ScienceDirect
Journal of Sound and Vibration 323 (2009) 662–676
JOURNAL OF SOUND AND VIBRATION
www.elsevier.com/locate/jsvi

An assessment of damping identification methods

Marco Prandina[a], John E. Mottershead[a,*], Elvio Bonisoli[b]

[a]*Department of Engineering, University of Liverpool, Brownlow Hill, Liverpool L69 3GH, UK*
[b]*Department of Production Systems, Politecnico di Torino, Corso Duca degli Abruzzi, 24-10129, Torino, Italy*

Received 18 September 2008; received in revised form 8 January 2009; accepted 13 January 2009
Handling Editor: C.L. Morfey
Available online 28 February 2009

Abstract

A study is carried out into the philosophy and performance of different approaches for the determination of linear viscous damping in elasto-mechanical systems. The methods studied include a closed-form solution, identification methods based on inverting the matrix of receptances, energy expressions developed from single-frequency excitation and responses as well as first-order perturbation methods. The work is concentrated particularly upon modal truncation and how this affects the distribution of matrix terms and the ability of the identified damping (together with known mass and stiffness terms) to reproduce the complex eigenvalues and eigenvectors of the full-order system. A simulated example is used to illustrate various points covered in the theoretical discussion of the methods considered.

1. Introduction

The oscillation of elasto-mechanical systems involves the exchange of kinetic and potential energies as well as the dissipation of energy by damping. Methods are generally well established for modelling the inertial and stiffness properties of most systems but often there remains very considerable doubt on how the damping behaviour should be represented. The most common method is to assume viscous damping, which is attractive computationally because it results in systems of second-order differential equations with solutions that are readily available by well-understood techniques. A regular approach is to simplify the assumption of viscous damping still further by selecting a damping matrix, $\mathbf{C}$, diagonalisable by the classical normal modes of the system, $\boldsymbol{\varphi}_j^T\mathbf{C}\boldsymbol{\varphi}_k = \delta_{jk}$. This form of damping, usually known as classical damping, includes proportional damping, $\mathbf{C} = \alpha\mathbf{M} + \beta\mathbf{K}$, as a special case. Necessary and sufficient conditions for classical damping, $\mathbf{K}\mathbf{M}^{-1}\mathbf{C} = \mathbf{C}\mathbf{M}^{-1}\mathbf{K}$, were established by Caughey [1,2].

The damping loss factor, defined by Crandall [3] to be the ratio of the energy dissipated in a cycle of single-frequency vibration to the peak potential energy stored in the system during the cycle, is a widely applied measure of the damping effect. Crandall [3] considered not only the classical viscous dashpot, but also the frequency dependent-dashpot, which includes as a special case the linear hysteretic damper, a well-known complication of which is the so-called 'non-equation' of mixed time and frequency domains resulting in non-causal behaviour in

*Corresponding author. Tel.: +44 0151 794 4827; fax: +44 0151 794 4848.
E-mail addresses: j.e.mottershead@liverpool.ac.uk, j.e.mottershead@liv.ac.uk (J.E. Mottershead).

0022-460X/$ - see front matter © 2009 Elsevier Ltd. All rights reserved.
doi:10.1016/j.jsv.2009.01.022

cases of impulsive or transient excitation. A very significant aspect of damping research has been the development of a range of mathematical models to represent a variety of damping mechanisms. A good appreciation of research into the damping behaviour of viscoelastic materials may be obtained from the survey carried out by Gaul [4], including (i) the use of fractional time derivatives to overcome problems of non-causality, (ii) wave propagation and transient vibration using integral transformation, and (iii) boundary element methods for solving damped 2D and 3D boundary value problems. Damping may also be significant in the joints of built-up structures, and often in such cases introduces nonlinearity into the system dynamics. In a recent study Jalali et al. [5] describe the identification of nonlinear damping (and stiffness) in a bolted joint and cite some 30 papers on the subject.

In this paper we are concerned with the performance of various damping identification methods. We concentrate solely upon general linear viscous damping and avoid the complications that might otherwise arise were we to consider other types of linear (and nonlinear) damping mechanisms. Therefore we choose not to use the damping loss factor, but instead to describe the dynamical system by using the symmetric state–space equation, usually attributed to Duncan (Fraser et al. [6]), and its behaviour in terms the resulting complex eigenvalues and eigenvectors. We mention as an aside that Staszewski [7] and Slavic et al. [8] describe a number of loss-factor identification procedures based on the continuous wavelet transform.

In non-classical viscous damping the eigenvectors are complex and the scaling of these modes generally causes a transfer of information between the real and imaginary parts. Ibrahim and Sestieri [9] introduced a normalisation that maximised the real parts and minimised the imaginary parts of the eigenvectors, thereby producing a modal mass matrix closest to the identity matrix. This result led to a measure of the difference between classical and general viscous damping models by Prells and Friswell [10] using an orthonormal matrix representing the phase between different degrees of freedom of the model. The matrix becomes the identity matrix when the damping is classical.

A closed-form solution for the damping matrix, as well as for the inverse mass and stiffness matrices and many other useful relationships was developed by Lancaster [11] using the theory of inverse lambda matrices [12]. Pilkey et al. [13] developed two methods, iterative and direct, based on Lancaster's closed-form solution for use with experimental modal data. Other methods for determining the damping matrix by identification include inversion of the matrix of frequency response functions (Chen et al. [14] and Lee and Kim [15]), energy methods involving integration over a period of single-frequency vibration (Liang [16]) and first-order perturbation as described by Adhikari and Woodhouse [17]. The latter paper was part of a series of papers by Adhikari and Woodhouse [17] on damping identification including linear viscous damping, non-viscous damping [18], symmetry preserving methods [19] and error analysis [20]. In a precursor to his papers with Adhikari, Woodhouse [21] had generalised the representation linear damping by a convolution integral, which reduces to linear viscous damping when the kernel functions are all delta functions multiplied by a symmetric matrix of coefficients.

A survey of damping identification methods has been carried out recently by Srikantha Phani and Woodhouse [22]. They studied the performance of a number of specific identification routines. Particular attention was paid to effect of contamination of frequency response function data by Gaussian random noise, the level of damping present (modal overlap), modal truncation of the data and spatial incompleteness.

In this paper we revisit the issue of determining damping models from experimental data. However, our study differs from the previous study [22] in a number of significant respects. (1) We concern ourselves mainly with the philosophy of the methods used and not so much with the performance of particular implementations and routines. (2) We do not repeat the previous work on noise contamination, the main reason for this being that noise contamination in frequency response functions is not Gaussian, indeed it is not entirely random. (3) Neither do we study the effect of an incomplete set of sensors. Rather than using model reduction or eigenvector expansion methods we consider the use of methods for the spatial location of the most significant damping terms to be a more fruitful approach and will report on this in a subsequent article.

The comparison of methods to be presented here will be focussed upon the effects of modal truncation. This is an inevitable consequence of modal testing over a limited frequency range and therefore worthy of further attention. Modal truncation was considered by Srikantha Phani and Woodhouse in their study [22], but a different method from the one presented here was used. In Ref. [22] a full-order damping matrix was identified and then transformed to modal coordinates, chosen modes were retained and others truncated, and finally the

transformation was reversed. It appears from their results that this procedure favoured the method of Adhikari and Woodhouse [17]. In the method presented here the truncation is applied directly and different results are obtained.

2. Preliminary calculations

We begin with the general second-order matrix differential equation

$$\mathbf{M}\ddot{\mathbf{x}}(t)+\mathbf{C}\dot{\mathbf{x}}(t)+\mathbf{K}\mathbf{x}(t)=\mathbf{f}(t) \tag{1}$$

$\mathbf{M},\mathbf{C},\mathbf{K}\in R^{n\times n}$, $\mathbf{M}=\mathbf{M}^{\mathrm{T}}$, $\mathbf{C}=\mathbf{C}^{\mathrm{T}}$, $\mathbf{K}=\mathbf{K}^{\mathrm{T}}$; $\mathbf{v}^{\mathrm{T}}\mathbf{M}\mathbf{v}>0$, $\mathbf{v}^{\mathrm{T}}\mathbf{C}\mathbf{v}\geqslant 0$, $\mathbf{v}^{\mathrm{T}}\mathbf{K}\mathbf{v}\geqslant 0$ for arbitrary $\mathbf{v}\neq\mathbf{0}$, $\mathbf{v}\in R^{n\times 1}$; and $\mathbf{x}$, $\mathbf{f}\in R^{n\times 1}$.

The dynamics of this system is governed by the second-order matrix pencil

$$P(s)=s^2\mathbf{M}+s\mathbf{C}+\mathbf{K} \tag{2}$$

the eigenvalues and eigenvectors of which satisfy the following equation:

$$P(\lambda_k)\boldsymbol{\psi}_k=\mathbf{0} \tag{3}$$

These eigenvalues and eigenvectors, forming self-conjugate sets, may be arranged to form the spectral and modal matrices

$$\begin{bmatrix}\boldsymbol{\Lambda} & \mathbf{0}\\ \mathbf{0} & \boldsymbol{\Lambda}^*\end{bmatrix}=\begin{bmatrix}\mathrm{diag}(\lambda_k) & \mathbf{0}\\ \mathbf{0} & \mathrm{diag}(\lambda_k^*)\end{bmatrix}\in C^{2n\times 2n} \tag{4}$$

$$[\boldsymbol{\Psi}\ \ \boldsymbol{\Psi}^*]=[\boldsymbol{\psi}_1\ldots\boldsymbol{\psi}_n\ \ \boldsymbol{\psi}_1^*\ldots\boldsymbol{\psi}_n^*]\in C^{n\times 2n} \tag{5}$$

Using the symmetric state–space arrangement [6] it is readily shown that

$$\begin{bmatrix}\boldsymbol{\Lambda}\boldsymbol{\Psi}^{\mathrm{T}} & \boldsymbol{\Psi}^{\mathrm{T}}\\ \boldsymbol{\Lambda}^*\boldsymbol{\Psi}^{*\mathrm{T}} & \boldsymbol{\Psi}^{*\mathrm{T}}\end{bmatrix}\left(s\begin{bmatrix}\mathbf{0} & \mathbf{M}\\ \mathbf{M} & \mathbf{C}\end{bmatrix}+\begin{bmatrix}-\mathbf{M} & \mathbf{0}\\ \mathbf{0} & \mathbf{K}\end{bmatrix}\right)\begin{bmatrix}\boldsymbol{\Psi}\boldsymbol{\Lambda} & \boldsymbol{\Psi}^*\boldsymbol{\Lambda}^*\\ \boldsymbol{\Psi} & \boldsymbol{\Psi}^*\end{bmatrix}=\begin{bmatrix}s\mathbf{I}-\boldsymbol{\Lambda} & \mathbf{0}\\ \mathbf{0} & s\mathbf{I}-\boldsymbol{\Lambda}^*\end{bmatrix} \tag{6}$$

where $\boldsymbol{\Psi}$ is normalised so that

$$\begin{bmatrix}\boldsymbol{\Lambda}\boldsymbol{\Psi}^{\mathrm{T}} & \boldsymbol{\Psi}^{\mathrm{T}}\\ \boldsymbol{\Lambda}^*\boldsymbol{\Psi}^{*\mathrm{T}} & \boldsymbol{\Psi}^{*\mathrm{T}}\end{bmatrix}\begin{bmatrix}\mathbf{0} & \mathbf{M}\\ \mathbf{M} & \mathbf{C}\end{bmatrix}\begin{bmatrix}\boldsymbol{\Psi}\boldsymbol{\Lambda} & \boldsymbol{\Psi}^*\boldsymbol{\Lambda}^*\\ \boldsymbol{\Psi} & \boldsymbol{\Psi}^*\end{bmatrix}=\mathbf{I}_{2n\times 2n} \tag{7}$$

$$\begin{bmatrix}\boldsymbol{\Lambda}\boldsymbol{\Psi}^{\mathrm{T}} & \boldsymbol{\Psi}^{\mathrm{T}}\\ \boldsymbol{\Lambda}^*\boldsymbol{\Psi}^{*\mathrm{T}} & \boldsymbol{\Psi}^{*\mathrm{T}}\end{bmatrix}\begin{bmatrix}-\mathbf{M} & \mathbf{0}\\ \mathbf{0} & \mathbf{K}\end{bmatrix}\begin{bmatrix}\boldsymbol{\Psi}\boldsymbol{\Lambda} & \boldsymbol{\Psi}^*\boldsymbol{\Lambda}^*\\ \boldsymbol{\Psi} & \boldsymbol{\Psi}^*\end{bmatrix}=-\begin{bmatrix}\boldsymbol{\Lambda} & \mathbf{0}\\ \mathbf{0} & \boldsymbol{\Lambda}^*\end{bmatrix} \tag{8}$$

Expanding Eqs. (7) and (8) leads to the orthogonality relationships given by Lancaster [11]

$$\begin{bmatrix}\boldsymbol{\Psi}^{\mathrm{T}}\\ \boldsymbol{\Psi}^{*\mathrm{T}}\end{bmatrix}\mathbf{M}[\boldsymbol{\Psi}\ \ \boldsymbol{\Psi}^*]\begin{bmatrix}\boldsymbol{\Lambda} & \\ & \boldsymbol{\Lambda}^*\end{bmatrix}+\begin{bmatrix}\boldsymbol{\Lambda} & \\ & \boldsymbol{\Lambda}^*\end{bmatrix}\begin{bmatrix}\boldsymbol{\Psi}^{\mathrm{T}}\\ \boldsymbol{\Psi}^{*\mathrm{T}}\end{bmatrix}\mathbf{M}[\boldsymbol{\Psi}\ \ \boldsymbol{\Psi}^*]+\begin{bmatrix}\boldsymbol{\Psi}^{\mathrm{T}}\\ \boldsymbol{\Psi}^{*\mathrm{T}}\end{bmatrix}\mathbf{C}[\boldsymbol{\Psi}\ \ \boldsymbol{\Psi}^*]=\mathbf{I}_{2n\times 2n} \tag{9}$$

$$-\begin{bmatrix}\boldsymbol{\Lambda} & \\ & \boldsymbol{\Lambda}^*\end{bmatrix}\begin{bmatrix}\boldsymbol{\Psi}^{\mathrm{T}}\\ \boldsymbol{\Psi}^{*\mathrm{T}}\end{bmatrix}\mathbf{M}[\boldsymbol{\Psi}\ \ \boldsymbol{\Psi}^*]\begin{bmatrix}\boldsymbol{\Lambda} & \\ & \boldsymbol{\Lambda}^*\end{bmatrix}+\begin{bmatrix}\boldsymbol{\Psi}^{\mathrm{T}}\\ \boldsymbol{\Psi}^{*\mathrm{T}}\end{bmatrix}\mathbf{K}[\boldsymbol{\Psi}\ \ \boldsymbol{\Psi}^*]=-\begin{bmatrix}\boldsymbol{\Lambda} & \\ & \boldsymbol{\Lambda}^*\end{bmatrix} \tag{10}$$

3. Lancaster's formula

Lancaster's formula [11] appeared in 1961 without proof, although a proof was given recently by Lancaster and Prells [23] using the theory of matrix polynomials. Alternatively, the formula can be developed from Eq. (7) in a few simple steps as will now be demonstrated.

By inverting Eq. (7) we find

$$\left(\begin{bmatrix} \mathbf{\Lambda\Psi}^{\mathrm{T}} & \mathbf{\Psi}^{\mathrm{T}} \\ \mathbf{\Lambda}^{*}\mathbf{\Psi}^{*\mathrm{T}} & \mathbf{\Psi}^{*\mathrm{T}} \end{bmatrix} \begin{bmatrix} \mathbf{0} & \mathbf{M} \\ \mathbf{M} & \mathbf{C} \end{bmatrix} \begin{bmatrix} \mathbf{\Psi\Lambda} & \mathbf{\Psi}^{*}\mathbf{\Lambda}^{*} \\ \mathbf{\Psi} & \mathbf{\Psi}^{*} \end{bmatrix}\right)^{-1} = \mathbf{I}_{2n\times 2n} \tag{11}$$

Expanding the inverse on the l.h.s. and rearranging leads to

$$\begin{bmatrix} \mathbf{0} & \mathbf{M} \\ \mathbf{M} & \mathbf{C} \end{bmatrix}^{-1} = \begin{bmatrix} \mathbf{\Psi\Lambda} & \mathbf{\Psi}^{*}\mathbf{\Lambda}^{*} \\ \mathbf{\Psi} & \mathbf{\Psi}^{*} \end{bmatrix} \begin{bmatrix} \mathbf{\Lambda\Psi}^{\mathrm{T}} & \mathbf{\Psi}^{\mathrm{T}} \\ \mathbf{\Lambda}^{*}\mathbf{\Psi}^{*\mathrm{T}} & \mathbf{\Psi}^{*\mathrm{T}} \end{bmatrix} \tag{12}$$

or

$$\begin{bmatrix} \mathbf{0} & \mathbf{M} \\ \mathbf{M} & \mathbf{C} \end{bmatrix}^{-1} = \begin{bmatrix} \mathbf{\Psi\Lambda}^{2}\mathbf{\Psi}^{\mathrm{T}} & \mathbf{\Psi\Lambda\Psi}^{\mathrm{T}} \\ \mathbf{\Psi\Lambda\Psi}^{\mathrm{T}} & \mathbf{0} \end{bmatrix} + \begin{bmatrix} \mathbf{\Psi}^{*}\mathbf{\Lambda}^{*2}\mathbf{\Psi}^{*\mathrm{T}} & \mathbf{\Psi}^{*}\mathbf{\Lambda}^{*}\mathbf{\Psi}^{*\mathrm{T}} \\ \mathbf{\Psi}^{*}\mathbf{\Lambda}^{*}\mathbf{\Psi}^{*\mathrm{T}} & \mathbf{0} \end{bmatrix} \tag{13}$$

It can be proven by application that the lhs matrix inverse is

$$\begin{bmatrix} \mathbf{0} & \mathbf{M} \\ \mathbf{M} & \mathbf{C} \end{bmatrix}^{-1} = \begin{bmatrix} -\mathbf{M}^{-1}\mathbf{C}\mathbf{M}^{-1} & \mathbf{M}^{-1} \\ \mathbf{M}^{-1} & \mathbf{0} \end{bmatrix} \tag{14}$$

By comparing the r.h.s matrices in Eqs. (13) and (14) it is seen that

$$-\mathbf{M}^{-1}\mathbf{C}\mathbf{M}^{-1} = \mathbf{\Psi\Lambda}^{2}\mathbf{\Psi}^{\mathrm{T}} + \mathbf{\Psi}^{*}\mathbf{\Lambda}^{*2}\mathbf{\Psi}^{*\mathrm{T}} \tag{15}$$

or

$$\mathbf{C} = -(\mathbf{M\Psi\Lambda}^{2}\mathbf{\Psi}^{\mathrm{T}}\mathbf{M} + \mathbf{M\Psi}^{*}\mathbf{\Lambda}^{*2}\mathbf{\Psi}^{*\mathrm{T}}\mathbf{M}) \tag{16}$$

which is Lancaster's formula. Expanding Eq. (16) leads to

$$\mathbf{C} = -\mathbf{M}\sum_{k}(\boldsymbol{\varphi}_{k}\lambda_{k}^{2}\boldsymbol{\varphi}_{k}^{\mathrm{T}} + \boldsymbol{\varphi}_{k}^{*}\lambda_{k}^{*2}\boldsymbol{\varphi}_{k}^{*\mathrm{T}})\mathbf{M} \tag{17}$$

or

$$\mathbf{C} = -2\mathbf{M}\sum_{k}\Re(\boldsymbol{\varphi}_{k}\lambda_{k}^{2}\boldsymbol{\varphi}_{k}^{\mathrm{T}})\mathbf{M} \tag{18}$$

Clearly the mass matrix must be known, but this may be an acceptable restriction, and we see that the damping matrix is constructed mode-by-mode. This means that if we know an incomplete set of eigenvalues and eigenvector corresponding to the limited frequency range of a vibration test and no others, then the same eigenvalues and eigenvectors will be returned exactly from Eq. (3) when $\mathbf{C}$ is computed using the truncated series in Eq. (18). The same equation ensures that the identified damping matrix is strictly real. Therefore the damping matrix $\mathbf{C}$ appears to be computed correctly by the truncated series for the frequency range in question and for example will reproduce exactly the modal damping ratios obtained in the test.

4. Damping matrix from the inverse receptance matrix

Lee and Kim [15] suggested that the viscous damping matrix might be obtained by inverting a measured receptance matrix and extracting the imaginary part. We write the receptance matrix in the form

$$\mathbf{H}(s) = \sum_{k=1}^{n}\left(\frac{\boldsymbol{\psi}_{k}\boldsymbol{\psi}_{k}^{\mathrm{T}}}{(s-\lambda_{k})} + \frac{\boldsymbol{\psi}_{k}^{*}\boldsymbol{\psi}_{k}^{*\mathrm{T}}}{(s-\lambda_{k}^{*})}\right) \tag{19}$$

and when $s = \mathrm{i}\omega$

$$\mathbf{H}(\mathrm{i}\omega) = \sum_{k=1}^{n}\left(\frac{\boldsymbol{\psi}_{k}\boldsymbol{\psi}_{k}^{\mathrm{T}}}{(\mathrm{i}\omega-\lambda_{k})} + \frac{\boldsymbol{\psi}_{k}^{*}\boldsymbol{\psi}_{k}^{*\mathrm{T}}}{(\mathrm{i}\omega-\lambda_{k}^{*})}\right) \tag{20}$$

or

$$\mathbf{H}(\mathrm{i}\omega) = \boldsymbol{\Psi}^{\mathrm{T}}(\mathrm{i}\omega\mathbf{I} - \boldsymbol{\Lambda})^{-1}\boldsymbol{\Psi} + \boldsymbol{\Psi}^{*\mathrm{T}}(\mathrm{i}\omega\mathbf{I} - \boldsymbol{\Lambda}^{*})^{-1}\boldsymbol{\Psi}^{*} \tag{21}$$

where

$$(\mathrm{i}\omega\mathbf{I} - \boldsymbol{\Lambda}) = \mathrm{diag}(\mathrm{i}\omega - \lambda_k) \tag{22}$$

We see that the receptance $\mathbf{H}(\mathrm{i}\omega)$ is dominated by the eigenvalues closest to the frequency ω.

Now consider the dynamic stiffness, expressed in state–space form

$$\mathbf{Z}'(\mathrm{i}\omega) = \begin{bmatrix} \mathbf{Z}'_{11}(\mathrm{i}\omega) & \mathbf{Z}'_{12}(\mathrm{i}\omega) \\ \mathbf{Z}'_{21}(\mathrm{i}\omega) & \mathbf{Z}'_{22}(\mathrm{i}\omega) \end{bmatrix} = \left(\mathrm{i}\omega \begin{bmatrix} \mathbf{0} & \mathbf{M} \\ \mathbf{M} & \mathbf{C} \end{bmatrix} + \begin{bmatrix} -\mathbf{M} & \mathbf{0} \\ \mathbf{0} & \mathbf{K} \end{bmatrix} \right) \tag{23}$$

and in terms of the modal and spectral matrices

$$\mathbf{Z}'(\mathrm{i}\omega) = \begin{bmatrix} \boldsymbol{\Lambda}\boldsymbol{\Psi}^{\mathrm{T}} & \boldsymbol{\Psi}^{\mathrm{T}} \\ \boldsymbol{\Lambda}^{*}\boldsymbol{\Psi}^{*\mathrm{T}} & \boldsymbol{\Psi}^{*\mathrm{T}} \end{bmatrix}^{-1} \begin{bmatrix} \mathrm{i}\omega\mathbf{I} - \boldsymbol{\Lambda} & \mathbf{0} \\ \mathbf{0} & \mathrm{i}\omega\mathbf{I} - \boldsymbol{\Lambda}^{*} \end{bmatrix} \begin{bmatrix} \boldsymbol{\Psi}\boldsymbol{\Lambda} & \boldsymbol{\Psi}^{*}\boldsymbol{\Lambda}^{*} \\ \boldsymbol{\Psi} & \boldsymbol{\Psi}^{*} \end{bmatrix}^{-1} \tag{24}$$

By combining Eqs. (24) and (7)

$$\mathbf{Z}'(\mathrm{i}\omega) = \begin{bmatrix} \mathbf{0} & \mathbf{M} \\ \mathbf{M} & \mathbf{C} \end{bmatrix} \begin{bmatrix} \boldsymbol{\Psi}\boldsymbol{\Lambda} & \boldsymbol{\Psi}^{*}\boldsymbol{\Lambda}^{*} \\ \boldsymbol{\Psi} & \boldsymbol{\Psi}^{*} \end{bmatrix} \begin{bmatrix} \mathrm{i}\omega\mathbf{I} - \boldsymbol{\Lambda} & \mathbf{0} \\ \mathbf{0} & \mathrm{i}\omega\mathbf{I} - \boldsymbol{\Lambda}^{*} \end{bmatrix} \begin{bmatrix} \boldsymbol{\Lambda}\boldsymbol{\Psi}^{\mathrm{T}} & \boldsymbol{\Psi}^{\mathrm{T}} \\ \boldsymbol{\Lambda}^{*}\boldsymbol{\Psi}^{*\mathrm{T}} & \boldsymbol{\Psi}^{*\mathrm{T}} \end{bmatrix} \begin{bmatrix} \mathbf{0} & \mathbf{M} \\ \mathbf{M} & \mathbf{C} \end{bmatrix} \tag{25}$$

so that

$$\mathbf{Z}(\mathrm{i}\omega) = -\omega^2\mathbf{M} + \mathrm{i}\omega\mathbf{C} + \mathbf{K} = \omega^2\mathbf{Z}'_{11}(\mathrm{i}\omega) + \mathbf{Z}'_{22}(\mathrm{i}\omega) \tag{26}$$

By expanding the product of the three central matrix terms of the right-hand side of Eq. (25) we find that

$$\begin{aligned} &\begin{bmatrix} \boldsymbol{\Psi}\boldsymbol{\Lambda} & \boldsymbol{\Psi}^{*}\boldsymbol{\Lambda}^{*} \\ \boldsymbol{\Psi} & \boldsymbol{\Psi}^{*} \end{bmatrix} \begin{bmatrix} \mathrm{i}\omega\mathbf{I} - \boldsymbol{\Lambda} & \mathbf{0} \\ \mathbf{0} & \mathrm{i}\omega\mathbf{I} - \boldsymbol{\Lambda}^{*} \end{bmatrix} \begin{bmatrix} \boldsymbol{\Lambda}\boldsymbol{\Psi}^{\mathrm{T}} & \boldsymbol{\Psi}^{\mathrm{T}} \\ \boldsymbol{\Lambda}^{*}\boldsymbol{\Psi}^{*\mathrm{T}} & \boldsymbol{\Psi}^{*\mathrm{T}} \end{bmatrix} \\ &= \begin{bmatrix} \sum_k (\boldsymbol{\psi}_k\lambda_k^2(\mathrm{i}\omega - \lambda_k)\boldsymbol{\psi}_k^{\mathrm{T}} + \boldsymbol{\psi}_k^{*}\lambda_k^{*2}(\mathrm{i}\omega - \lambda_k^{*})\boldsymbol{\psi}_k^{*T}) & \sum_k (\boldsymbol{\psi}_k\lambda_k(\mathrm{i}\omega - \lambda_k)\boldsymbol{\psi}_k^{\mathrm{T}} + \boldsymbol{\psi}_k^{*}\lambda_k^{*}(\mathrm{i}\omega - \lambda_k^{*})\boldsymbol{\psi}_k^{*\mathrm{T}}) \\ \sum_k (\boldsymbol{\psi}_k\lambda_k(\mathrm{i}\omega - \lambda_k)\boldsymbol{\psi}_k^{\mathrm{T}} + \boldsymbol{\psi}_k^{*}\lambda_k^{*}(\mathrm{i}\omega - \lambda_k^{*})\boldsymbol{\psi}_k^{*\mathrm{T}}) & \sum_k (\boldsymbol{\psi}_k(\mathrm{i}\omega - \lambda_k)\boldsymbol{\psi}_k^{\mathrm{T}} + \boldsymbol{\psi}_k^{*}(\mathrm{i}\omega - \lambda_k^{*})\boldsymbol{\psi}_k^{*\mathrm{T}}) \end{bmatrix} \end{aligned} \tag{27}$$

We see that the contribution of the kth mode vanishes as $\mathrm{i}\omega$ approaches λ_k and the high-frequency poles become very significant through squaring in the upper right-hand sub-matrix. Thus the low-frequency $\mathbf{Z}(\mathrm{i}\omega)$ is dominated by the high-frequency eigenvalues far away from the frequency ω. Berman [24,25] explained the meaning of this result, that it is impossible to invert a receptance matrix of a practical structure with many modes, measured over a limited frequency range, in order to estimate the matrices $\mathbf{M}$, $\mathbf{C}$, $\mathbf{K}$. Consequently, a damping matrix identified by extracting the imaginary part of an inverted matrix of measured receptances will only be correct if all the modes are present in the measurements. This is possible in simulation but never happens in the practical case of mechanical systems with distributed mass and stiffness.

In the case when fewer than a full complement of modes are present, the matrix product

$$\begin{bmatrix} \boldsymbol{\Lambda}\boldsymbol{\Psi}^{\mathrm{T}} & \boldsymbol{\Psi}^{\mathrm{T}} \\ \boldsymbol{\Lambda}^{*}\boldsymbol{\Psi}^{*\mathrm{T}} & \boldsymbol{\Psi}^{*\mathrm{T}} \end{bmatrix} \begin{bmatrix} \mathbf{0} & \mathbf{M} \\ \mathbf{M} & \mathbf{C} \end{bmatrix}$$

is precisely the pseudo inverse of

$$\begin{bmatrix} \boldsymbol{\Psi}\boldsymbol{\Lambda} & \boldsymbol{\Psi}^{*}\boldsymbol{\Lambda}^{*} \\ \boldsymbol{\Psi} & \boldsymbol{\Psi}^{*} \end{bmatrix}.$$

It is convenient here to express the pseudo inverse in terms of $\mathbf{M}$ and $\mathbf{C}$ only because it enables us to draw conclusions on the contributions of the modes, as in the previous paragraph. In practice the measured receptance matrix would be ill-conditioned (close to singularity except for the presence of noise) and should be

inverted directly, typically using singular value decomposition and omitting the contributions of the smallest singular values. It is seen from Eqs. (25)–(27) that the dynamic stiffness matrix is built up mode-by-mode and therefore it is to be expected that the identified damping **C**, when combined with **M** and **K**, will accurately reproduce the complex eigenvalues of the system. The damping matrix, **C**, is obtained together with **M** and **K** when the matrix of receptances is inverted, then **C** is assumed to be given from the imaginary part, but there is no constraint that prevents **C** (or for that matter **M** or **K**) from being complex.

5. Energy dissipation using single-frequency time-domain responses

An energy equation may be obtained by pre-multiplying the equation of motion by $\dot{\mathbf{x}}^{\mathrm{T}}$, applying a single-frequency input and integrating over one period. Using an approach that differs slightly from Liang [16], we write

$$\int_t^{t+T} \dot{\mathbf{x}}^{\mathrm{T}}(\mathbf{M}\ddot{\mathbf{x}} + \mathbf{K}\mathbf{x} + \mathbf{F}(\mathbf{x}, \dot{\mathbf{x}}))\,\mathrm{d}t = \int_t^{t+T} \dot{\mathbf{x}}^{\mathrm{T}}\mathbf{f}(t)\,\mathrm{d}t \tag{28}$$

where it is seen that the damping $\mathbf{F}(\mathbf{x}, \dot{\mathbf{x}})$ offers no limitation to viscous, or indeed to any linear or nonlinear form of damping. For the purposes of discussion we will restrict ourselves to linear viscous damping.

By integrating over a single period (or an integer multiple of the period) it is found that the conservative terms vanish, leaving the expression,

$$\int_t^{t+T} \dot{\mathbf{x}}^{\mathrm{T}}\mathbf{C}\dot{\mathbf{x}}\,\mathrm{d}t = \int_t^{t+T} \dot{\mathbf{x}}^{\mathrm{T}}\mathbf{f}\,\mathrm{d}t \tag{29}$$

where

$$\mathbf{f}(t) = \begin{pmatrix} f_1 \\ f_2 \\ \vdots \\ f_n \end{pmatrix} \cos\,\omega t \tag{30}$$

and

$$\dot{\mathbf{x}}(t) = -\omega \begin{pmatrix} \Re(x_1) \\ \Re(x_2) \\ \vdots \\ \Re(x_n) \end{pmatrix} \sin\,\omega t + \omega \begin{pmatrix} \Im(x_1) \\ \Im(x_2) \\ \vdots \\ \Im(x_n) \end{pmatrix} \cos\,\omega t \tag{31}$$

or in condensed form

$$\dot{\mathbf{x}}(t) = -\omega \begin{pmatrix} a_1 \\ a_2 \\ \vdots \\ a_n \end{pmatrix} \sin\,\omega t + \omega \begin{pmatrix} b_1 \\ b_2 \\ \vdots \\ b_n \end{pmatrix} \cos\,\omega t = -\omega\mathbf{a}\,\sin\,\omega t + \omega\mathbf{b}\,\cos\,\omega t \tag{32}$$

Now

$$\dot{\mathbf{x}}^{\mathrm{T}}\mathbf{C}\dot{\mathbf{x}} = \mathbf{a}^{\mathrm{T}}\omega^2\mathbf{C}\mathbf{a}\sin^2(\omega t) - \mathbf{a}^{\mathrm{T}}\omega^2\mathbf{C}\mathbf{b}\,\sin(\omega t)\cos(\omega t) - \mathbf{b}^{\mathrm{T}}\omega^2\mathbf{C}\mathbf{a}\,\sin(\omega t)\cos(\omega t) + \mathbf{b}^{\mathrm{T}}\omega^2\mathbf{C}\mathbf{b}\cos^2(\omega t) \tag{33}$$

$$\dot{\mathbf{x}}^{\mathrm{T}}\mathbf{f} = -\omega\mathbf{a}^{\mathrm{T}}\mathbf{f}\,\sin(\omega t)\cos(\omega t) + \omega\mathbf{b}^{\mathrm{T}}\mathbf{f}\cos^2(\omega t) \tag{34}$$

and since

$$\int_0^{2\pi} \cos^2(\omega t)\,\mathrm{d}(\omega t) = \int_0^{2\pi} \sin^2(\omega t)\,\mathrm{d}(\omega t) = \pi \tag{35}$$

$$\int_0^{2\pi} \cos(\omega t)\sin(\omega t)\,\mathrm{d}(\omega t) = 0 \tag{36}$$

then Eq. (29) may be cast in the simplified form

$$\mathbf{a}^{\mathrm{T}}(\omega\mathbf{C})\mathbf{a} + \mathbf{b}^{\mathrm{T}}(\omega\mathbf{C})\mathbf{b} = \mathbf{b}^{\mathrm{T}}\mathbf{f} \tag{37}$$

In principle the solution of Eq. (37) for $\mathbf{C}$ using different force configurations at the same frequency—to give an overdetermined system—provides exactly the same solution as inverting $\mathbf{H}(\mathrm{i}\omega)$ in the previous section. In Appendix A we show how the energy Eq. (37) may be obtained directly from the receptance matrix and its inverse.

For the good performance of the energy method the modes of the structure must be present in the data over a sufficiently wide range of frequencies as described exactly in the previous section. The energy method, as described above, does not operate using the modes of the system and therefore knowledge of the mass matrix is not a requirement.

Of course the overdetermined system of equations developed from Eq. (37) may include many different single-frequency responses, which would be beneficial in practical application. Equally, in the previous section $\mathbf{C}$ may be estimated from an overdetermined system of equations formed from receptance matrices at many different frequencies as described by Lee and Kim [15].

6. Damping by first-order perturbation analysis

The following expressions were originally developed by Lord Rayleigh [26] and have been re-iterated in recent times by Lees [27] and Adhikari and Woodhouse [17]:

$$\lambda_k, \lambda_k^* = -\frac{\boldsymbol{\varphi}_k^{\mathrm{T}}\mathbf{C}\boldsymbol{\varphi}_k}{2} \pm \mathrm{i}\omega_k \tag{38}$$

$$\boldsymbol{\psi}_k, \boldsymbol{\psi}_k^* = \boldsymbol{\varphi}_k \pm \mathrm{i}\omega_k \sum_j \frac{\boldsymbol{\varphi}_k^{\mathrm{T}}\mathbf{C}\boldsymbol{\varphi}_j}{\omega_k^2 - \omega_j^2}\boldsymbol{\varphi}_j \tag{39}$$

In these equations the undamped eigenvalues and eigenvectors are denoted ω_k and $\boldsymbol{\varphi}_k$, the latter normalised using the undamped orthogonality condition $\boldsymbol{\varphi}_k^{\mathrm{T}}\mathbf{M}\boldsymbol{\varphi}_j = \delta_{kj}$. The damping is such that the damped eigenvalues and eigenvectors λ_k and $\boldsymbol{\psi}_k$ differ from ω_k and $\boldsymbol{\varphi}_k$ by a small amount.

Adhikari and Woodhouse develop their method as follows:

(1) Define $\Re(\boldsymbol{\Psi}) = \boldsymbol{\Phi} = \mathbf{U}$, $\Im(\boldsymbol{\Psi}) = \mathbf{V}$ and assume the columns of $\mathbf{V}$ to be given by a linear combination of the columns of $\mathbf{U}$, so that

$$\mathbf{V} = \mathbf{U}\mathbf{B} \tag{40}$$

and

$$\mathbf{B} = (\mathbf{U}^{\mathrm{T}}\mathbf{U})^{-1}\mathbf{U}^{\mathrm{T}}\mathbf{V} \tag{41}$$

for an incomplete set of frequencies and modes. The terms in $\mathbf{U}$ and $\mathbf{V}$ are directly the measured real and imaginary parts of the complex eigenvectors.

(2) It can be seen from Eqs. (39) and (40) that

$$c'_{jk} = \boldsymbol{\varphi}_k^{\mathrm{T}}\mathbf{C}\boldsymbol{\varphi}_j = \frac{(\omega_k^2 - \omega_j^2)b_{jk}}{\omega_k}; \quad j \neq k \tag{42}$$

and from Eq. (38)

$$c'_{kk} = \boldsymbol{\varphi}_k^{\mathrm{T}} \mathbf{C} \boldsymbol{\varphi}_k = 2\Re(\lambda_k) \tag{43}$$

Eqs. (42) and (43) complete the matrix $\mathbf{C}'$, which is the fully populated damping matrix in the modal coordinates of the undamped system.

(3) The matrix $\mathbf{C}$ is now computed as

$$\mathbf{C} = \mathbf{U}(\mathbf{U}^{\mathrm{T}}\mathbf{U})^{-1}\mathbf{C}'(\mathbf{U}^{\mathrm{T}}\mathbf{U})^{-1}\mathbf{U}^{\mathrm{T}} \tag{44}$$

It is seen that the matrices $\mathbf{C}$ and $\mathbf{C}'$ are generally not symmetric. Adhikari and Woodhouse [19] modified their formulation by placing a constraint on the solution of $\mathbf{B}$ that ensured a symmetric solution for $\mathbf{C}'$ and hence for $\mathbf{C}$.

The method depends upon pseudo inversions of the undamped eigenvectors $\mathbf{U}$ in Eqs. (41) and (44). By combining Eqs. (35) and (36) we obtain the projection of $\mathbf{V}$ onto the columns of $\mathbf{U}$. Thus,

$$\mathbf{U}(\mathbf{U}^{\mathrm{T}}\mathbf{U})^{-1}\mathbf{U}^{\mathrm{T}}\mathbf{V} = \mathbf{V}' \neq \mathbf{V} \tag{45}$$

This means that the matrix $\mathbf{B}$ obtained from Eq. (41) results in the projection $\mathbf{V}'$ when substituted into Eq. (40). The error $\mathbf{E} = (\mathbf{V} - \mathbf{V}')$ is therefore carried into Eq. (41) which in turn produces erroneous values for $\mathbf{C}'$. The Frobenius norm of this error $||\mathbf{E}||_F/||\mathbf{V}||_F \times 100\%$ may be used as an indicator to assess whether or not enough modes have been included in $\mathbf{U}$ and $\mathbf{V}$.

In Eq. (44) pseudo inverses are used in the transformation from modal to physical coordinates, of $\mathbf{C}'$ to $\mathbf{C}$. If we pre- and post-multiply Eq. (44) by $\mathbf{U}^{\mathrm{T}}$ and $\mathbf{U}$, thereby reversing the transformation, then

$$\mathbf{U}^{\mathrm{T}}\mathbf{U}(\mathbf{U}^{\mathrm{T}}\mathbf{U})^{-1}\mathbf{C}'(\mathbf{U}^{\mathrm{T}}\mathbf{U})^{-1}\mathbf{U}^{\mathrm{T}}\mathbf{U} = \mathbf{C}' \tag{46}$$

We see at once that if the damping matrix in modal coordinates $\mathbf{C}'$ is known exactly it is converted to physical coordinates with perfect accuracy by Eq. (44). Thus it is the pseudo inverse in Eq. (41) that introduces errors into the damping estimate and not the pseudo inversions in Eq. (44).

Since Eqs. (38) and (39) are developed using the undamped orthogonality equation, it is clear that the first-order perturbation method requires a known mass matrix, as indeed does Lancaster's method.

7. Numerical example: cantilever beam with three dashpots

We use the numerical example of the cantilever beam shown in Fig. 1 to illustrate the various points made in the analysis above. The beam, of length 0.56 m and cross section 0.04 m (breadth) × 0.004 m (depth) has the standard material properties of aluminium. In-plane bending vibrations are considered. Grounded dashpots are connected at coordinates 3, 13 and 17 with damping coefficients of 0.2, 0.5 and 0.15 Ns/m respectively. The beam model consists of ten Euler–Bernoulli beams, having twenty coordinates and the same number of damped modes of vibration.

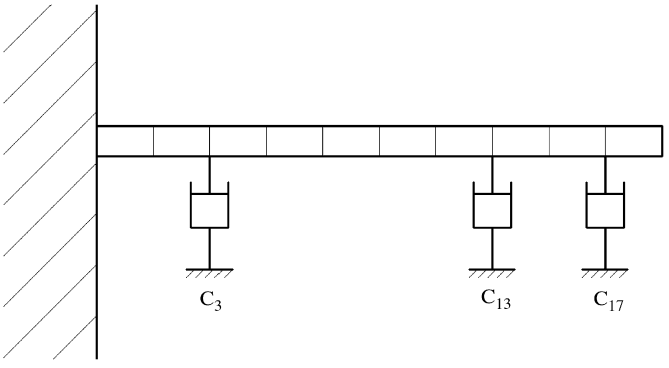

Fig. 1. Finite element cantilever beam with three dashpots.

7.1. Accuracy of eigenvalue and eigenvector calculations

One way of assessing the effectiveness of the identified damping matrix is to compute the eigenvalues of the system, using the known **M** and **K** and the identified **C**. Natural frequencies and modal damping ratios determined for the computed eigenvalues are listed in Tables 1 and 2 using the identified damping matrix from data consisting of five measured modes. All three methods (Lancaster's formula, inverting $\mathbf{H}(i\omega)$ and

Table 1
Natural frequencies (rad/s) (five measured modes).

Mode	Exact	Lancaster	Inverse of $\mathbf{H}(i\omega)$	Perturbation
1	65.45	65.45	65.45	65.45
2	410.16	410.16	410.16	410.16
3	1148.71	1148.71	1148.71	1148.71
4	2252.59	2252.59	2252.59	2252.60
5	3729.53	3729.53	3729.53	3729.53
6	5587.26	5587.26	5587.26	5587.31
7	7839.20	7839.20	7839.20	7839.24
8	10,502.37	10,502.37	10,502.37	10,502.46
9	13,579.43	13,579.43	13,579.43	13,579.51
10	16,881.19	16,881.19	16,881.19	16,881.35
11	22,468.11	22,468.12	22,468.11	22,468.32
12	27,144.31	27,144.30	27,144.31	27,145.03
13	32,905.22	32,905.22	32,905.22	32,906.51
14	39,714.40	39,714.40	39,714.40	39,718.82
15	47722.70	47,722.70	47,722.70	47,743.74
16	57,076.72	57,076.73	57,076.73	57,189.76
17	67,741.22	67,741.23	67,741.22	67,789.80
18	79084.58	79,084.65	79,084.63	79,272.22
19	89,058.18	89,058.08	89,058.11	88,698.73
20	111,455.14	111,455.07	111,455.15	111,265.52

Table 2
Damping ratios (five measured modes).

Mode	Exact	Lancaster	Inverse of $\mathbf{H}(i\omega)$	Perturbation
1	0.036247	0.036247	0.036247	0.036247
2	0.002208	0.002208	0.002208	0.002208
3	0.002140	0.002140	0.002140	0.002140
4	0.000711	0.000711	0.000711	0.000711
5	0.000281	0.000281	0.000281	0.000281
6	0.000433	0.000000	0.000000	0.000553
7	0.000243	0.000000	0.000000	0.000292
8	0.000097	0.000000	0.000000	0.000301
9	0.000224	0.000000	0.000000	0.000201
10	0.000186	0.000000	0.000000	0.000195
11	0.000022	0.000000	0.000000	0.000171
12	0.000027	0.000000	0.000000	0.000304
13	0.000066	0.000000	0.000000	0.000428
14	0.000031	0.000000	0.000000	0.000729
15	0.000027	0.000000	0.000000	0.002977
16	0.000040	0.000000	0.000000	0.009675
17	0.000015	0.000000	0.000000	0.004627
18	0.000004	0.000000	0.000000	0.004859
19	0.000004	0.000000	0.000000	0.134941
20	0.000006	0.000000	0.000000	0.007014

first-order perturbation) produce estimates very close to the exact natural frequencies. In Table 2 all three methods return estimated damping ratios that exactly reproduce the exact damping ratios for the first five modes. Since the data is restricted to the first five modes, the remaining modes should be undamped. It is seen that Lancaster's formula and inverse $\mathbf{H}(i\omega)$ do indeed correctly reproduce the undamped modes. The perturbation method identifies damping in modes 6–20 that should not be present.

The modes determined from the identified $\mathbf{C}$ and those with exact damping are compared using a generalised MAC correlation

$$\mathrm{MAC}(j,k)=\frac{\left|\begin{bmatrix}\lambda_k\boldsymbol{\psi}_k\\ \boldsymbol{\psi}_k\end{bmatrix}^{\mathrm{T}}\mathbf{W}_j\begin{bmatrix}\lambda_j\boldsymbol{\psi}_j\\ \boldsymbol{\psi}_j\end{bmatrix}\begin{bmatrix}\lambda_j\boldsymbol{\psi}_j\\ \boldsymbol{\psi}_j\end{bmatrix}^{\mathrm{T}}\mathbf{W}_k\begin{bmatrix}\lambda_k\boldsymbol{\psi}_k\\ \boldsymbol{\psi}_k\end{bmatrix}\right|}{\left|\begin{bmatrix}\lambda_j\boldsymbol{\psi}_j\\ \boldsymbol{\psi}_j\end{bmatrix}^{\mathrm{T}}\mathbf{W}_j\begin{bmatrix}\lambda_j\boldsymbol{\psi}_j\\ \boldsymbol{\psi}_j\end{bmatrix}\begin{bmatrix}\lambda_k\boldsymbol{\psi}_k\\ \boldsymbol{\psi}_k\end{bmatrix}^{\mathrm{T}}\mathbf{W}_k\begin{bmatrix}\lambda_k\boldsymbol{\psi}_k\\ \boldsymbol{\psi}_k\end{bmatrix}\right|} \tag{47}$$

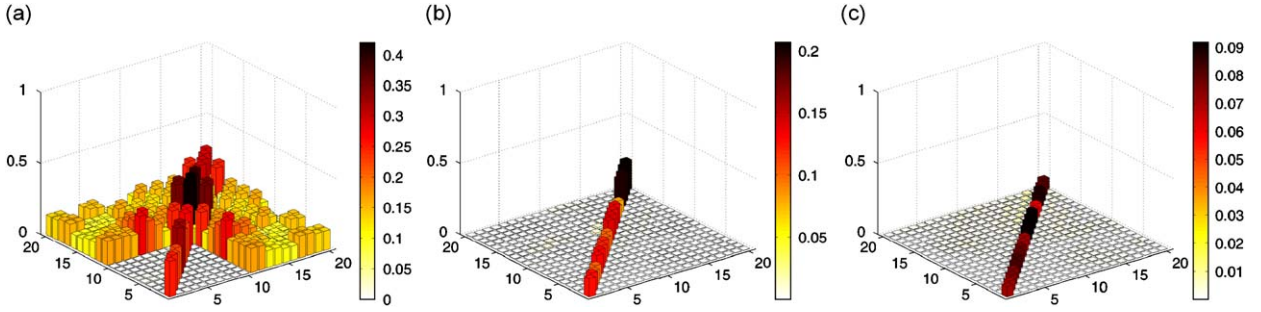

Fig. 2. $\boldsymbol{\eta}$-array—Lancaster's formula using: (a) 5 modes, (b) 10 modes and (c) 15 modes.

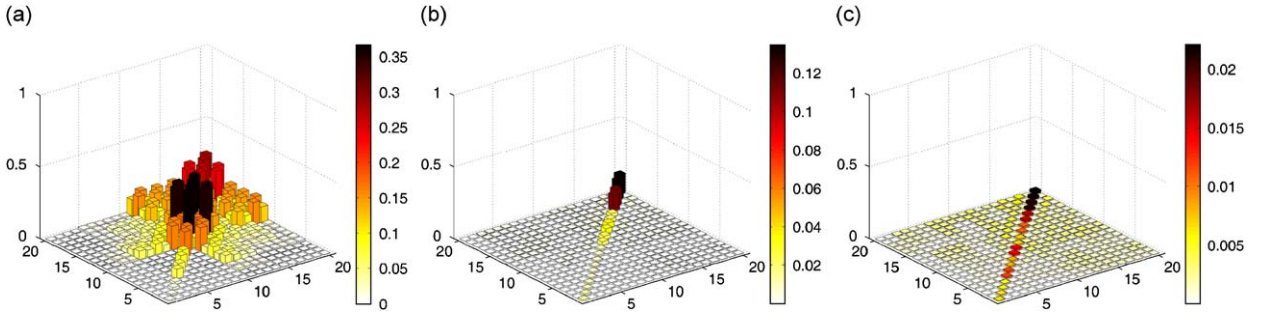

Fig. 3. $\boldsymbol{\eta}$-array—inversion of $\mathbf{H}(i\omega)$ using: (a) 5 modes, (b) 10 modes and (c) 15 modes.

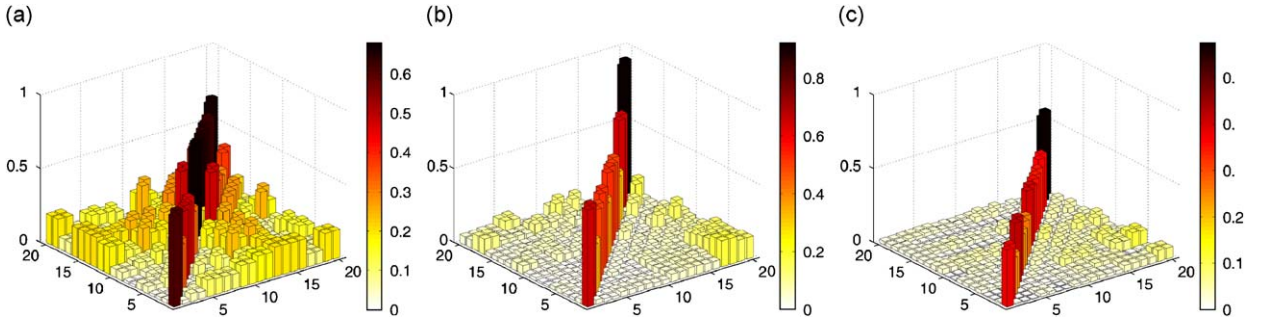

Fig. 4. $\boldsymbol{\eta}$-array—first-order perturbation using: (a) 5 modes, (b) 10 modes and (c) 15 modes.

where the modal weight is given by

$$\mathbf{W}_i = |\lambda_i| \begin{bmatrix} \mathbf{0} & \mathbf{M} \\ \mathbf{M} & \tilde{\mathbf{C}} \end{bmatrix} + \begin{bmatrix} -\mathbf{M} & \mathbf{0} \\ \mathbf{0} & \mathbf{K} \end{bmatrix} \tag{48}$$

and $\tilde{\mathbf{C}}$ is the identified damping matrix. The modal properties for the identified $\tilde{\mathbf{C}}$ and the exact $\mathbf{C}$ are denoted by the subscripts j and k, respectively. This generalised MAC returns an identity matrix when $\tilde{\mathbf{C}} = \mathbf{C}$. We take the array given by

$$\boldsymbol{\eta} = |\mathbf{I} - \mathbf{MAC}| \tag{49}$$

which results in the null matrix for exact damping identification.

The $\boldsymbol{\eta}$ arrays computed with different numbers of measured modes are shown in Figs. 2–4. The inverse $\mathbf{H}(i\omega)$ consistently returns the most accurate eigenvectors and the least accurate are those given by first-order perturbation. It is seen that inverting $\mathbf{H}(i\omega)$ returns the first five eigenvectors with excellent accuracy even when only five modes are measured.

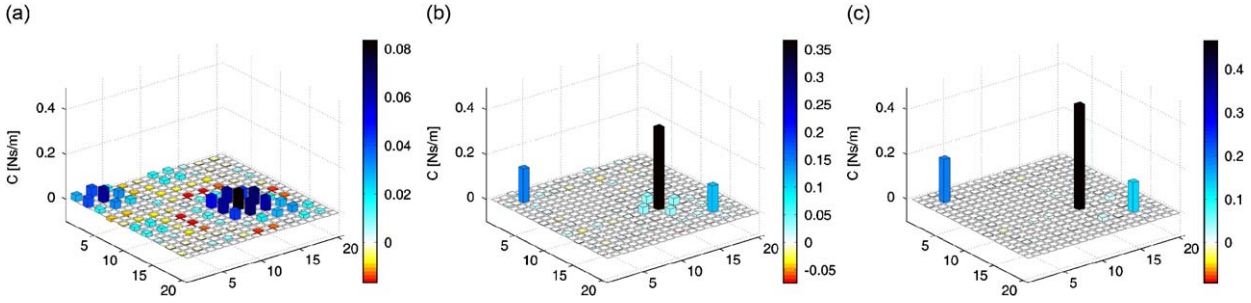

Fig. 5. Identified damping coefficients—Lancaster's formula using: (a) 5 modes, (b) 10 modes and (c) 15 modes.

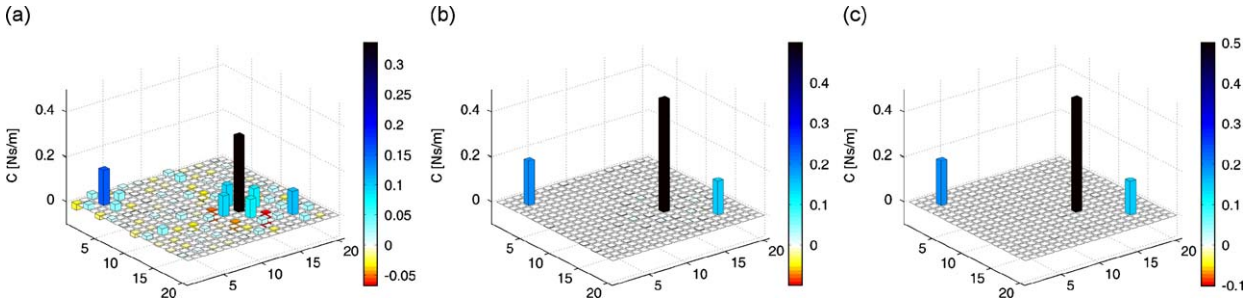

Fig. 6. Identified damping coefficients—inversion of $\mathbf{H}(i\omega)$ using: (a) 5 modes, (b) 10 modes and (c) 15 modes.

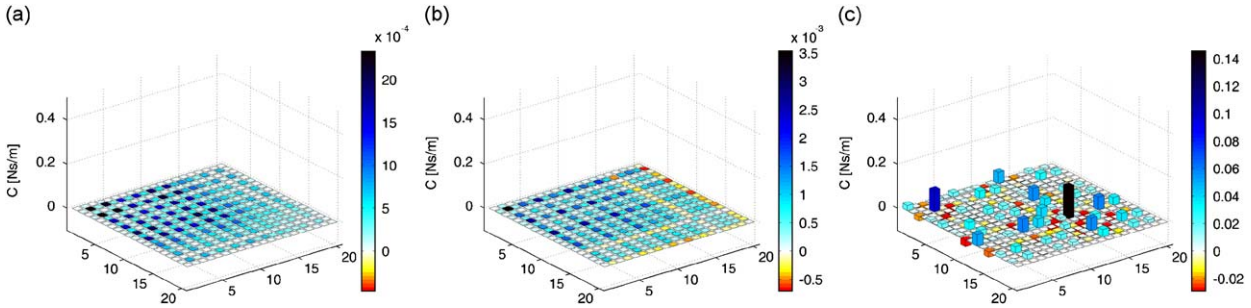

Fig. 7. Identified damping coefficients—first-order perturbation using: (a) 5 modes, (b) 10 modes and (c) 15 modes.

7.2. Accuracy of the identified matrix of damping coefficients **C**

The contents of the identified damping matrix determined by the three methods using different numbers of measured modes are shown in Figs. 5–7. It is seen that inverting $\mathbf{H}(i\omega)$ produces three prominent peaks at the correct locations of the grounded dampers, coordinates 3, 13 and 17, even when only five modes are measured. Very accurate representation of the damping matrix is obtained using 10 modes. Lancaster's formula also produces a good estimate of **C**, but not quite as good as the inverse $\mathbf{H}(i\omega)$ method. The first-order perturbation method results in a fully populated damping matrix with the damping distributed over almost all of the system coordinates. It is seen in Fig. 7 that the identified damping terms are very small for the cases of 5 and 10 measured modes. Figs. 5–7 are all shown with the same scale on the vertical axis. When 15 modes are measured prominent peaks begin to appear at coordinates 3 and 13.

The error in the damping matrix is assessed in Fig. 8 using the formula $\varepsilon_C = ||\mathbf{C} - \tilde{\mathbf{C}}||_F / ||\mathbf{C}||_F \times 100\%$. It is seen that the inverse $\mathbf{H}(i\omega)$ method converges most rapidly. All three methods converge to the correct damping matrix when all the modes are available for measurement. The first-order perturbation approach is investigated further in Fig. 9 where the projection error, $||\mathbf{E}||_F / ||\mathbf{V}||_F \times 100\%$, described in Section 6, is shown

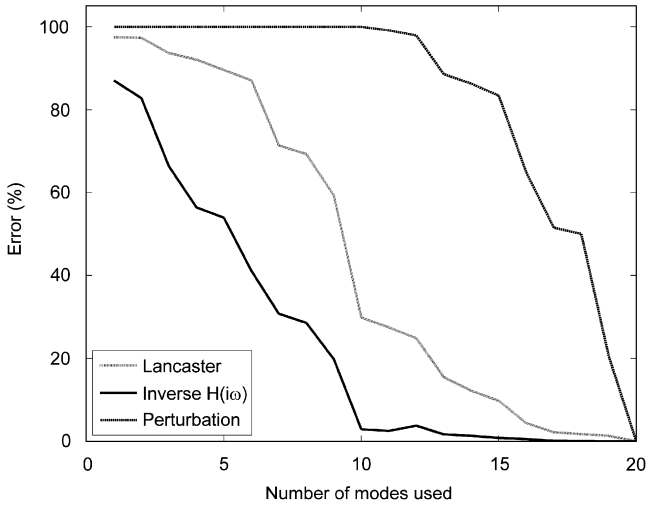

Fig. 8. Error ε_C for the three methods.

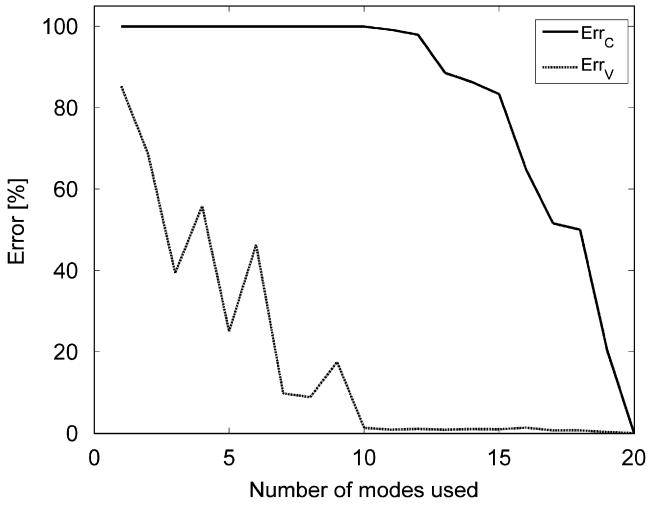

Fig. 9. Error by first-order perturbation.

together with ε_C. Even when the projection error is reduced to a very small amount, when 10 or more modes are measured, a significant error persists in the terms of the damping matrix and their distribution on the beam.

In Section 4 we referred to the problem of inverting $\mathbf{H}(i\omega)$ to determine the dynamic stiffness matrix $\mathbf{Z}(i\omega)$. This problem is illustrated in Figs. 10 and 11, which show the receptances and dynamic stiffnesses obtained from Eqs. (20) and (25)–(27), respectively, for the cases of 5, 10, 15 and 20 measured modes. As expected the low-frequency receptances are accurately represented even when only a small sub-set of modes are measured. Conversely, reasonably accurate low-frequency dynamic stiffnesses are only available when fifteen or more modes are measured. Despite this limitation the best estimate of the damping matrix is consistently obtained by inverting $\mathbf{H}(i\omega)$. We note that by Lancaster's formula the damping matrix is strictly real and determined separately from the other system matrices $\mathbf{M}$ and $\mathbf{K}$. On the other hand, by inverting $\mathbf{H}(i\omega)$, the dynamic stiffness, $\mathbf{Z}(i\omega)$, is determined which includes $\mathbf{M}$, $\mathbf{C}$ and $\mathbf{K}$ together. When the measured modes are incomplete no constraint is placed on the method to ensure that the system matrices are strictly real. Thus, taking the

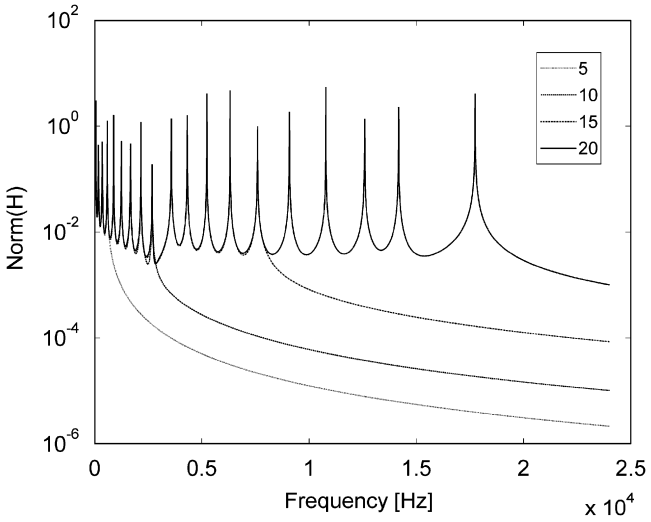

Fig. 10. Receptances determined from an incomplete set of modes.

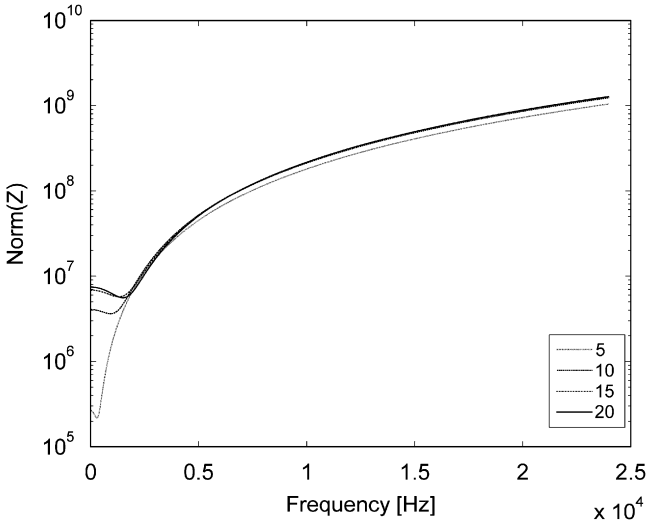

Fig. 11. Dynamic stiffnesses determined from an incomplete set of modes.

imaginary part of $\mathbf{H}^{-1}(\mathrm{i}\omega)$ allows greater freedom than is available by Lancaster's formula. This additional freedom accounts for the superior performance of the inverse $\mathbf{H}(\mathrm{i}\omega)$ method over the other two methods.

8. Conclusions

Of the methods studied there are essentially three fundamentally different approaches; the closed-form solution developed by Lancaster [11], methods based on inverting the measured matrix of receptances, typically Lee and Kim [15] (which are equivalent, in the case of linear viscous damping, to single-frequency energy methods, typically Liang [16]) and first-order perturbation as described by Adhikari and Woodhouse [17]. All three approaches are found to be capable of closely reproducing the complex eigenvalues within the frequency range of data obtained by modal truncation. Lancaster's formula and the inverse $\mathbf{H}(\mathrm{i}\omega)$ method correctly return eigenvalues with zero modal damping corresponding to the truncated modes. However, first-order perturbation includes some erroneous residual damping seen in the truncated modes that should correctly be undamped. This turns out to be a significant indicator of the poorer performance of the perturbation method in locating the damping terms correctly in the matrix. It is also the least accurate method for determining the complex eigenvectors. The best performing method is inverse $\mathbf{H}(\mathrm{i}\omega)$ and its superiority over the closed-form solution is attributed to the extra flexibility of the method—whereas Lancaster's solution restricts the damping matrix to real solutions, the inverse $\mathbf{H}(\mathrm{i}\omega)$ method places no such restriction on the system matrices $\mathbf{M}$, $\mathbf{C}$, $\mathbf{K}$ but simply takes the imaginary part of the complex dynamic stiffness $\mathbf{Z}(\mathrm{i}\omega)$.

Acknowledgement

This work is funded by the European Union for the Marie Curie Excellence Team ECERTA under contract number MEXT-CT-2006 042383.

Appendix A. Energy equation from the receptance matrix

We begin with Eq. (37) and suppose now that, $\mathbf{f} = \mathbf{e}_i$ where $\mathbf{e}_i$ is the ith column of the identity matrix. The response to this ith force input may then be expressed as

$$\mathbf{x}_i = \begin{pmatrix} h_{1i} \\ h_{2i} \\ \vdots \\ h_{ni} \end{pmatrix}; \quad \mathbf{a}_i = \Re \begin{pmatrix} h_{1i} \\ h_{2i} \\ \vdots \\ h_{ni} \end{pmatrix}; \quad \mathbf{b}_i = \Im \begin{pmatrix} h_{1i} \\ h_{2i} \\ \vdots \\ h_{ni} \end{pmatrix} \tag{A.1}$$

Now we may re-write Eq. (37) as

$$\mathbf{a}_i^{\mathrm{T}}(\omega\mathbf{C})\mathbf{a}_i + \mathbf{b}_i^{\mathrm{T}}(\omega\mathbf{C})\mathbf{b}_i = \mathbf{b}_i^{\mathrm{T}}\mathbf{e}_i \tag{A.2}$$

Also from the receptance matrix, by definition

$$(\Re(\mathbf{H}^{-1}) + \mathrm{i}\Im(\mathbf{H}^{-1}))\Re(\mathbf{H}) + \mathrm{i}\Im(\mathbf{H})) = \mathbf{I} \tag{A.3}$$

so that

$$\Re(\mathbf{H}^{-1})\mathbf{a}_i - \Im(\mathbf{H}^{-1})\mathbf{b}_i = \mathbf{e}_i \tag{A.4}$$

$$\Re(\mathbf{H}^{-1})\mathbf{b}_i + \Im(\mathbf{H}^{-1})\mathbf{a}_i = \mathbf{0} \tag{A.5}$$

and

$$-\omega^2\mathbf{M} + \mathbf{K} = \Re(\mathbf{H}^{-1}(\mathrm{i}\omega)) \tag{A.6}$$

$$\omega\mathbf{C} = \Im(\mathbf{H}^{-1}(\mathrm{i}\omega)) \tag{A.7}$$

Eqs. (A.4) and (A.5) may be cast as

$$(-\omega^2\mathbf{M}+\mathbf{K})\mathbf{a}_i-(\omega\mathbf{C})\mathbf{b}_i=\mathbf{e}_i \tag{A.8}$$

$$(\omega\mathbf{C})\mathbf{a}_i+(-\omega^2\mathbf{M}+\mathbf{K})\mathbf{b}_i=\mathbf{0} \tag{A.9}$$

From Eq. (A.9)

$$\mathbf{b}_i=-(-\omega^2\mathbf{M}+\mathbf{K})^{-1}(\omega\mathbf{C})\mathbf{a}_i \tag{A.10}$$

and by premultiplying Eq. (A.8) by $\mathbf{b}_i^{\mathrm{T}}$ and combining with (A.10), we finally obtain from the receptance matrix

$$\mathbf{a}_i^{\mathrm{T}}(\omega\mathbf{C})\mathbf{a}_i+\mathbf{b}_i^{\mathrm{T}}(\omega\mathbf{C})\mathbf{b}_i=\mathbf{b}_i^{\mathrm{T}}\mathbf{e}_i \tag{A.11}$$

which is the same as Eq. (A.2) from energy considerations.

References

[1] T.K. Caughey, Classical normal modes in damped linear systems, *ASME Journal of Applied Mechanics* 27 (1960) 269–271.
[2] T.K. Caughey, M.E.J. O'Kelly, Classical normal modes in damped linear systems, *ASME Journal of Applied Mechanics* 32 (1965) 583–588.
[3] S.H. Crandall, The role of damping in vibration theory, *Journal of Sound and Vibration* 11 (1) (1970) 3–18.
[4] L. Gaul, The influence of damping on waves and vibrations, *Mechanical Systems and Signal Processing* 13 (1) (1999) 1–30.
[5] H. Jalali, H. Ahmadian, J.E. Mottershead, Identification of nonlinear bolted lap-joint parameters by force-state mapping, *International Journal of Solids and Structures* 44 (25–26) (2007) 8087–8105.
[6] R.A. Frazer, W.J. Duncan, A.R. Collar, *Elementary Matrices*, Cambridge University Press, Cambridge, 1946.
[7] W.J. Staszewski, Identification of damping in MDOF systems using time-scale decomposition, *Journal of Sound and Vibration* 203 (2) (1997) 283–305.
[8] J. Slavic, I. Simonovski, M. Boltezar, Damping identification using a continuous wavelet transform: application to real data, *Journal of Sound and Vibration* 262 (2003) 291–307.
[9] S.R. Ibrahim, A. Sestieri, Existence and normalisation of complex modes in post experimental modal analysis, *Proceedings of the 13th IMAC,* Nashville TN, 1995, pp. 483–489.
[10] U. Prells, M.I. Friswell, A measure of non-proportional damping, *Mechanical Systems and Signal Processing* 14 (2) (2000) 125–137.
[11] P. Lancaster, Expression of damping matrices in linear vibrations problems, *Journal of the Aerospace Sciences* 28 (1961) 256.
[12] P. Lancaster, Inversion of lambda-matrices and application to the theory of vibration, *Archive for Rational Mechanics and Analysis* 6 (2) (1960) 105–114.
[13] D.F. Pilkey, G. Park, D.J. Inman, Damping matrix identification and experimental verification, *Proceedings of the Sixth SPIE Symposium on Smart Structures and Materials*, Newport Beach, CA, 1999, pp. 350–357.
[14] S.Y. Chen, M.S. Ju, Y.G. Tsuei, Estimation of mass, stiffness and damping matrices from frequency response functions, *ASME Journal of Vibration and Acoustics* 118 (1996) 78–82.
[15] J.-H. Lee, J. Kim, Development and validation of a new experimental method to identify damping matrices of a dynamic system, *Journal of Sound and Vibration* 246 (30) (2001) 505–524.
[16] J.-W. Liang, Damping estimation via energy dissipation method, *Journal of sound and Vibration* 307 (2007) 349–364.
[17] S. Adhikari, J. Woodhouse, Identification of damping: part 1, viscous damping, *Journal of Sound and Vibration* 243 (1) (2001) 43–61.
[18] S. Adhikari, J. Woodhouse, Identification of damping: part 2, non-viscous damping, *Journal of Sound and Vibration* 243 (1) (2001) 63–88.
[19] S. Adhikari, J. Woodhouse, Identification of damping: part 3, symmetry-preserving methods, *Journal of Sound and Vibration* 251 (2001) 477–490.
[20] S. Adhikari, J. Woodhouse, Identification of damping: part 4, error analysis, *Journal of Sound and Vibration* 251 (2001) 491–504.
[21] J. Woodhouse, Linear damping models for structural vibration, *Journal of Sound and Vibration* 215 (3) (1998) 547–569.
[22] A. Srikantha Phani, J. Woodhouse, Viscous damping identification in linear vibration, *Journal of Sound and Vibration* 303 (2006) 475–500.
[23] P. Lancaster, U. Prells, Inverse problems for damped vibrating systems, *Journal of Sound and Vibration* 283 (2005) 891–914.
[24] A. Berman, A.W.G. Flannelly, Theory of incomplete models of dynamic structures, *AIAA Journal* 9 (8) (1971) 1481–1487.
[25] A. Berman, System identification of structural dynamic models—theoretical and practical bounds, AIAA Conference paper 84-0929, 1984.
[26] L. Rayleigh, Theory of Sound, Dover, New York, 1945 (reissued).
[27] A.W. Lees, Use of perturbation analysis for complex modes, *Proceedings of the 17th IMAC*, 1999, pp. 779–784.